J|A|C|S COMMUNICATIONS

Published on Web 07/29/2010

Multicompartment Core/Shell Microgels

Xiaobo Hu,[†,‡] Zhen Tong,[‡] and L. Andrew Lyon*[,†]

School of Chemistry & Biochemistry and the Petit Institute for Bioengineering and Bioscience, Georgia Institute of Technology, Atlanta, Georgia 30332, and Research Institute of Material Science, South China University of Technology, Guangzhou 510640, P. R. China

Received June 26, 2010; E-mail: lyon@gatech.edu

Abstract: Multiresponsive poly(*N*-isopropylacrylamide-*co*-acrylic acid) (pNIPAm-AAc) microgels containing mechanically and thermodynamically decoupled poly(*N*-isopropylmethacrylamide) (pNIPMAm) cores have been prepared. To achieve this structure, pNIPMAm microgels were used as templates in the synthesis of an *N*,*N*′-(1,2-dihydroxyethylene)bisacrylamide (DHEA) cross-linked pNIPMAm inner shell. A pNIPAm-AAc outer shell was then added, resulting in "core/double-shell" microgels. Erosion of the inner shell via periodate-mediated cleavage of the 1,2-diol bond in DHEA produced multiresponsive core/shell microgels with independent cores. The striking structural changes and unique multiresponsivity achieved in microgels prepared via this approach illustrate the potential of multifunctional, multicomponent delivery vehicles that do not suffer from antagonistic interferences arising when different functional components are introduced within a single particle.

Nanomaterials designed to interface with biological systems comprise a continually expanding area of research. Of particular interest are colloidal particles with core/shell or core/corona structures. From simple poly(ethyleneglycol)-modified liposomes to more advanced multiblock copolymer micelles, such structures offer the promise of controlled (shell-mediated) biological interactions plus excellent carrier (core-based) properties.[1] We and others have employed this design in the fabrication of core/shell (CS) hydrogel particles (microgels and nanogels), which have stimulated interest in fields such as drug delivery,[2,3] biosensing,[4,5] chemical separations,[6] and catalysis.[7]

In principle, one might naïvely expect the CS strategy to permit independent tuning of the core and shell properties. In reality, mechanical coupling between the core and shell influences the physicochemical properties of the two components.[8−12] This is particularly true for responsive particles, such as those containing the common thermoresponsive polymer poly(*N*-isopropylacrylamide) (pNIPAm). In these particles, mechanical CS coupling leads to thermodynamic coupling, where core desolvation can impact the swelling of the shell and vice versa.[8−11,13] Thus, the independent tuning model for CS materials fails under these conditions.

Recently, "yolk/shell" structured particles have been developed to impart a physical separation between the core and shell in inorganic colloids.[14,15] We have taken inspiration from those efforts in the preparation of multicompartment CS microgels. The synthesis of core/double-shell (CDS) microgels is shown schematically in Figure 1. Core particles (C) composed of *N*,*N*′-methylenebis(acrylamide) (BIS) cross-linked pNIPMAm were prepared by free-radical precipitation polymerization. The core served as a seed for the subsequent polymerization of an *N*,*N*′-(1,2-dihydroxyethylene)bisacrylamide (DHEA) cross-linked pNIPMAm shell, resulting in CS microgels. CS microgels were then used as nuclei for the addition of a BIS cross-linked poly(*N*-isopropylacrylamide-*co*-acrylic acid) (pNIPAm-AAc) shell, resulting in CDS microgels.

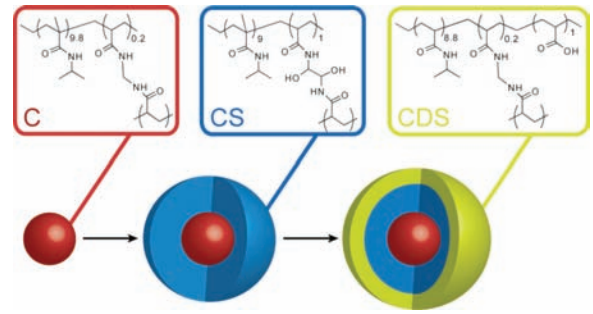

Figure 1. Schematic depiction of the synthetic approach used in the synthesis of core/double-shell microgels.

DHEA contains a 1,2-glycol bond that can be cleaved by $NaIO_4$, permitting shell dissolution (see Figure S1c, Supporting Information);[16] periodate-triggered erosion of the inner shell is shown schematically in Figure 2a. The result is a degraded core/double-shell (CDS-D) microgel with a decoupled core and outer shell. Figure 2b shows atomic force microscopy (AFM) height and phase images and line profiles of CDS microgels before periodate treatment. The microgels appear monodispersed and spherical, with a taller feature at the particle center. Presumably, this feature corresponds to the pNIPMAm core and inner shell. Particle heights were ∼30 nm, which is taller than the ∼23 nm height measured for the core microgels (Figure S1a), thus indicating successful shell addition.

Not surprisingly, CDS-D microgels have a very different morphology than CDS microgels (Figure 2c). Without the connectivity of the inner shell, the outer shell appears to have less structural rigidity, spreading dramatically on the substrate during the drying process. Indeed, the shell is now so flat that it is barely observable in the height image at the scale presented. The phase image, however, clearly illustrates the presence of the outer shell. Note also that the pNIPMAm cores are no longer located exactly in the centers of the particles. This is especially true when the microgels are absorbed and dried from pH 6.5 buffer (Figure S1d). This observation is suggestive of mechanical decoupling of the core and outer shell, which is accompanied by free movement of the core.

To further establish the formation of CDS-D microgels, we employed fluorescence spectroscopy.[16] The DHEA cross-linked pNIPMAm shell was tagged with a 4-acrylamidofluorescein. The fluorescein-labeled CS and CDS microgels show characteristic

[†] Georgia Institute of Technology.
[‡] South China University of Technology.

10.1021/ja105616v

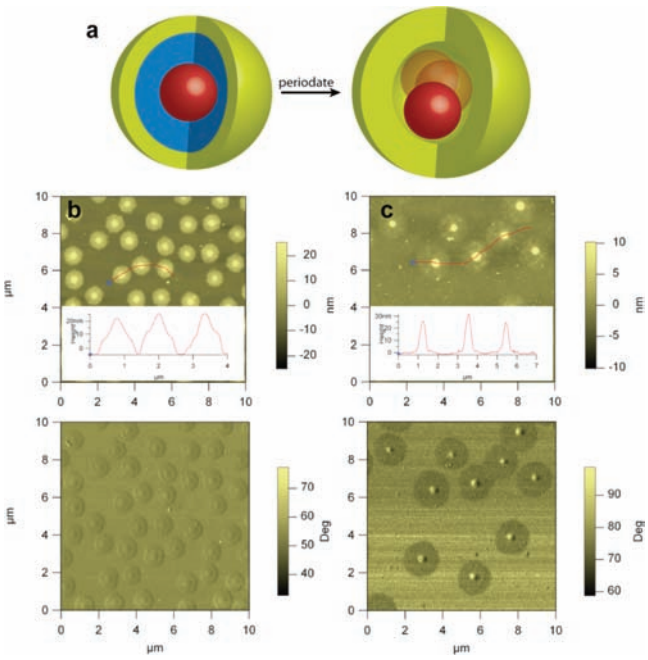

Figure 2. (a) Schematic depiction of CDS-D microgel formation by degradation and solubilization of the inner shell. AFM height and phase images and line profiles of (b) CDS and (c) CDS-D microgels adsorbed and dried on glass substrates from microgel dispersions prepared in deionized water. Scans are 10 × 10 μm.

emission spectra, with an emission peak centered at 515 nm upon excitation at 493 nm (Figure 3). Following periodate treatment and purification via centrifugation, the emission peak is no longer observed, indicating shell removal from both CS-D and CDS-D microgels.

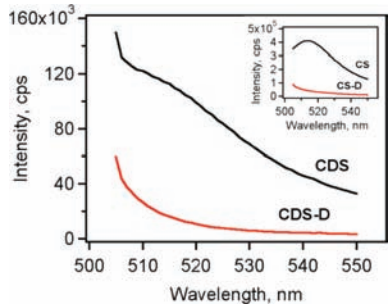

Figure 3. Fluorescence spectra (λ_{ex} = 493 nm) of CDS and CDS-D microgels. Inset: spectra of CS and CS-D microgels.

In addition to changes in structure/morphology and composition, the erosion of the inner shell should impact the thermodynamic coupling of the core and outer shell. Such coupling should be evident in the microgel pH- and thermo-responsivity, which we have studied by photon correlation spectroscopy (PCS). The successful addition of a shell at each step can also be confirmed by the increase of the microgel size in the collapsed state (Figure 4 and Figure S2, Supporting Information). Figure 4a shows a pNIPMAm core volume phase transition temperature (VPTT) of ~43 °C at pH 3, which is consistent with the lower critical solution temperature of pNIPMAm. At this pH, CDS particles display two distinct transitions, with one at ~31 °C resulting from the collapse of the pNIPAm-AAc outer shell and the other at ~42 °C due to the collapse of the pNIPMAm-based core and inner shell. These two transitions can also be observed from changes in scattering intensity as a function of temperature (Figure S3, Supporting Information). These two transitions are still observed following periodate treatment and inner shell removal, with only slight changes observed in the particle sizes in the swollen and deswollen states. At temperatures below the first transition, the radius of CDS-D microgels is slightly larger than that of the CDS microgels, presumably due to decreased connectivity; this has been observed previously in the fabrication of hollow microgels.[16] It is interesting to note that core collapse for CDS-D microgels at pH 3 is accompanied by a decrease in the overall size of the microgel, despite the shell having already collapsed at a lower temperature. This is due to the swollen core preventing the shell from complete collapse at temperatures lower than ~43 °C. Upon core deswelling, further shell collapse is then permitted, resulting in an overall particle size decrease. Additionally, a decrease in microgel size is observed in the fully deswollen state, which likely arises from the decrease in segment density following shell removal.

The impact of inner shell removal is more apparent when the shell-localized AAc groups are deprotonated. At pH 6.5, the CDS microgels swell to ~390 nm due to AAc deprotonation and the associated increase in osmotic pressure.[17,18] At ~50 °C, a small decrease in size is observed, which is likely due to hindered collapse of the acid-free core.[13] Following inner shell removal, the CDS-D microgels swell more than 150 nm in radius to ~540 nm. Importantly, the thermally induced collapse observed for the CDS particles is now absent, with the CDS-D particle radius being temperature independent at pH 6.5. This observation is in stark contrast, however, to what is observed in the scattering intensity (Figure 4c). An increase in scattering is observed at ~44 °C for both the CDS and CDS-D microgels, indicating collapse of the pNIPMAm-based core. Indeed, following inner shell removal, the increase in scattering is ~1.5-fold larger than that for the CDS particle, suggesting unhindered deswelling of the core component. The fact that core deswelling is observable via light scattering intensity, but is not apparent in the overall particle size, is a clear indication of mechanical and thermodynamic decoupling of the microgel core and shell.

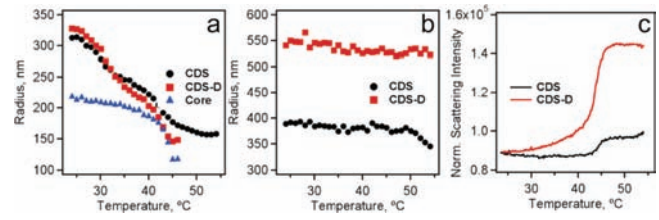

Figure 4. CDS and CDS-D microgel radii as a function of temperature in (a) pH 3 and (b) pH 6.5 buffers. (c) Light scattering intensity as a function of temperature at pH 6.5. The core data are shown in panel (a) for comparison. All buffers have an ionic strength of 10 mM.

In summary, we have demonstrated a practical route to the synthesis of multicompartment microgels containing a pNIPMAm core displaying mechanical and thermodyanamic independence from the outer pNIPAm-AAc shell. Presumably the core and shell components are separated by a low polymer density or polymer-free aqueous region. Such structures, which contain an amphiphilic, thermo-responsive region (the core), an interstitial aqueous region, and a pH- and thermo-responsive shell, suggest opportunities for multicomponent encapsulation and release strategies wherein the particle−biology interface (the shell) remains unperturbed by the properties, contents, or responsivity of the core. This kind of architectural control allows for the rational design of multifunctional, multicomponent colloids without concern over antagonistic effects that may occur between the different components.

Acknowledgment. X.H. thanks China Scholarship Council (CSC) for financial support.

Supporting Information Available: Experimental procedures, AFM images, and light scattering data for intermediate particle structures. This material is available free of charge via the Internet at http://pubs.acs.org.

References

(1) Nayak, S.; Lyon, L. A. *Angew. Chem., Int. Ed.* **2005**, *44*, 7686–7708.
(2) Blackburn, W. H.; Dickerson, E. B.; Smith, M. H.; McDonald, J. F.; Lyon, L. A. *Bioconjugate Chem.* **2009**, *20*, 960–968.
(3) Gu, J. X.; Xia, F.; Wu, Y.; Qu, X. Z.; Yang, Z. Z.; Jiang, L. *J. Controlled Release* **2007**, *117*, 396–402.
(4) Lapeyre, V.; Renaudie, N.; Dechezelles, J. F.; Saadaoui, H.; Ravaine, S.; Ravaine, V. *Langmuir* **2009**, *25*, 4659–4667.
(5) Luo, Q. F.; Liu, P. X.; Guan, Y.; Zhang, Y. J. *ACS Appl. Mater. Interfaces* 20102, 760–767.
(6) Nayak, S.; Lyon, L. A. *Angew. Chem., Int. Ed.* **2004**, *43*, 6706–6709.
(7) Lu, Y.; Mei, Y.; Drechsler, M.; Ballauff, M. *Angew. Chem., Int. Ed.* **2006**, *45*, 813–816.
(8) Jones, C. D.; McGrath, J. G.; Lyon, L. A. *J. Phys. Chem. B* **2004**, *108*, 12652–12657.
(9) Jones, C. D.; Lyon, L. A. *Langmuir* **2003**, *19*, 4544–4547.
(10) Berndt, I.; Popescu, C.; Wortmann, F. J.; Richtering, W. *Angew. Chem., Int. Ed.* **2006**, *45*, 1081–1085.
(11) Berndt, I.; Pedersen, J. S.; Richtering, W. *J. Am. Chem. Soc.* **2005**, *127*, 9372–9373.
(12) Christodoulakis, K. E.; Vamvakaki, M. *Langmuir* **2010**, *26*, 639–647.
(13) Jones, C. D.; Lyon, L. A. *Macromolecules* **2000**, *33*, 8301–8306.
(14) Kamata, K.; Lu, Y.; Xia, Y. N. *J. Am. Chem. Soc.* **2003**, *125*, 2384–2385.
(15) Wu, X. J.; Xu, D. S. *J. Am. Chem. Soc.* **2009**, *131*, 2774–2775.
(16) Nayak, S.; Gan, D. J.; Serpe, M. J.; Lyon, L. A. *Small* **2005**, *1*, 416–421.
(17) Dai, S.; Ravi, P.; Tam, K. C. *Soft Matter* **2008**, *4*, 435–449.
(18) Tan, B. H.; Tam, K. C. *Adv. Colloid Interface Sci.* **2008**, *136*, 25–44.

JA105616V